

Aerobic Alcohol Oxidations Mediated by Nitric Acid**

Christof Aellig, Christophe Girard, and Ive Hermans*

The selective oxidation of organic substrates plays a pivotal role in the chemical value-chain.^[1,2] Despite the industrial relevance, the scientific understanding of oxyfunctionalization technologies lags behind the current state-of-the-art. Radical-chain autoxidations are a classical example of large-scale technology which is still not completely understood.^[3] Nitric acid based oxidations are another example of poorly understood processes of tremendous industrial importance.^[2a,4] The production of adipic acid (3 Mt/year)—a building block for nylon-6,6—from a mixture of cyclohexanol/cyclohexanone, the synthesis of glyoxylic acid (80 kt/year)—used in the synthesis of vanillin and Amoxicillin—as well as the oxidation of dimethyldisulfide to methanesulfonic acid (30 kt/year)—used in electroplating and detergent formulations—are just a few examples from bulk and commodity chemistry.^[1,2a,5] However, oxidations with nitric acid are also extensively used for the synthesis of fine-chemicals.^[6] The reason why HNO₃-based oxidations are so valuable is the fact that nitric acid is an inexpensive oxidant that can achieve remarkable selectivities. One disadvantage of this technology is the strongly acidic nature of nitric acid, especially when applied in high concentration. Another disadvantage is the stoichiometric reduction of the HNO₃ to NO_x and N₂O. In a large-scale process (such as adipic acid synthesis),^[7] NO_x and N₂O are separated, and the NO_x is recycled into nitric acid. This ex situ NO_x recycling however results in large recycle streams. Moreover, on a smaller scale—such as typically encountered in fine-chemical industry—it usually does not pay to recycle the NO_x. Nitrous oxide, being a severe greenhouse gas, cannot be recycled and should be (catalytically) decomposed prior to emission.^[1] More recently, N₂O arising from adipic acid production has also been used to oxidize olefins to valuable ketone products.^[1,8] To date the formation mechanism of N₂O in nitric acid based oxidations has not been elucidated, making it a difficult to decrease its formation.

Recently, aerobic oxidation reactions which use sub-stoichiometric amounts of HNO₃ have been proposed.^[9–11] In those systems, strong acids (such as hydrochloric acid), or carbon-based materials (such as active carbon), are added to achieve a catalytic turnover in HNO₃. Although the reaction mechanism is currently unknown, the idea is very attractive.

The final goal would be to develop a process which uses nitric acid as an oxygen carrier in which O₂ is the true terminal oxidant. However, the proposed systems suffer from various shortcomings, such as limited turnover. In addition, HCl leads to corrosive reaction conditions and poses recycling issues; highly dispersed carbon-based materials do not seem very appealing as oxidation catalysts from a stability or even safety point of view.

Herein, the aerobic oxidation of benzyl alcohol (PhCH₂OH) to benzaldehyde (PhCHO), by HNO₃, is investigated. This partial oxidation is not only a model reaction of interest to (fine-)chemical synthesis,^[12] the selectivity of this reaction is also very sensitive to radical side-reactions which easily cause over-oxidation of PhCHO to benzoic acid (PhCOOH).^[13] Selective aerobic alcohol oxidations with catalytic amounts of HNO₃ could offer an attractive metal-free alternative to precious-metal-catalyzed systems.

To investigate the HNO₃-based PhCH₂OH oxidation and to decouple the dual role of HNO₃—being both an oxidant and a strong acid—sub-stoichiometric amounts of HNO₃ were used in the presence of a solid acid as (co-)catalyst. Screening of various solid acids, including most conventional zeolites (e.g., MFI, BEA, FAU, and MOR topologies), revealed the ion-exchange resin amberlyst-15 in protonic form (4.7 meqg⁻¹) as a promising candidate. Actually, zeolites gave disappointing results, probably due to strong sorption of HNO₃ and NO_x species, inhibiting the reaction. Our standard experiments are performed in a bubble column reactor using 25 mL 1,4-dioxane as solvent, [PhCH₂OH]₀ = 500 mM, [HNO₃]₀ = 125 mM, 150 mg of amberlyst-15 (corresponding to [H⁺]_{amberlyst} = 28 mM), and 1 atm of O₂ (bubbling through at 100 mL min⁻¹). An induction period was observed which could be eliminated by the addition of small amounts of NaNO₂ (Figure 1, curves a–c). This observation—known from

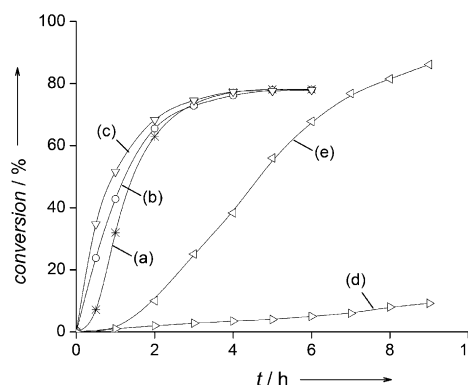


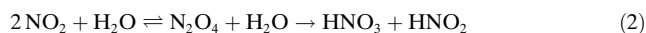
Figure 1. Effect of the NaNO₂ concentration on the PhCH₂OH conversion at 80 °C: a–c) at 1 atm O₂ (0, 5, and 15 mM NaNO₂, respectively); d, e) at 20 atm O₂ (0 and 5 mM NaNO₂, respectively).

[*] C. Aellig, C. Girard, Prof. Dr. I. Hermans
 ETH Zurich, Institute for Chemical and Bioengineering
 Wolfgang-Pauli-Strasse 10, CH-8093 Zurich (Switzerland)
 E-mail: hermans@chem.ethz.ch
 Homepage: <http://www.hermans.ethz.ch>

[**] We acknowledge the financial support from ETH Zurich (grant ETH-18 09-2).

Supporting information for this article is available on the WWW under <http://dx.doi.org/10.1002/anie.201105620>.

the literature^[12]—points towards the crucial role of HNO_2 , which is formed upon protonation of NO_2^- . Inhibition of the reaction in the presence of urea—a known HNO_2 trap^[14]—is in line with this hypothesis. NO and NO_2 can alternatively be used to shorten the induction period (see Supporting Information), pointing towards an efficient interconversion of the nitrogen species.^[15] Interesting to note is that under N_2 bubbling (1 atm) at 80°C , the conversion levels off after 6 h to 50%, leading to a $\Delta[\text{PhCH}_2\text{OH}]/[\text{HNO}_3]_0 \approx 2$. Under the same conditions, but in presence of 1 atm O_2 , a conversion of 80% can be achieved in 6 h (see curve b in Figure 1). Nevertheless, the initial reaction rate is approximately 40% lower in the presence of O_2 , compared to N_2 (see Supporting Information). These observations indicate that oxygen plays an ambiguous role in this system. On the one hand O_2 is able to trigger a recycling of the active species and thereby increase the final conversion, on the other hand it reduces the reaction rate. At elevated O_2 pressures (e.g., 20 atm in a high-pressure autoclave) the induction period is significantly longer than at atmospheric pressure, even in presence of initiator (Figure 1, curves e and d). This elongated induction period is probably caused by a shift of the equilibrated decomposition of HNO_3 to NO_2 towards the left-hand-side at higher O_2 pressure [Reaction (1)]. Indeed, NO_2 is able to form HNO_2 by Reaction (2),^[4,16] the key oxidizing species in the system, and a shift of the equilibrium in Reaction (1) will hence reduce the HNO_2 concentration. Note that the amberlyst catalyst accelerates the HNO_3 decomposition to NO_2 (see Supporting Information), thereby speeding up the formation of active species.



Gas–liquid mass transfer is found to play an important role for this reaction: when the reaction is performed under a static O_2 pressure (in a round-bottom flask with an oxygen balloon, conventional lab practice), the end conversion is 20% lower than in a bubble column at the same pressure but with enhanced gas–liquid mass-transfer.

The reaction is quasi first-order in HNO_3 , although the initial rate is clearly leveling off at increasing $[\text{HNO}_3]_0$ (see Supporting Information). This observation points towards an initiating role of nitric acid, rather than a pure stoichiometric reaction. The reaction rate is proportional to the amberlyst loading, up to 4 mg mL^{-1} after which it levels off (Figure 2). Although this could in principle point towards gas–liquid mass-transfer limiting the reaction, an alternative mechanistic explanation is proposed below. Fluid–solid mass-transfer effects can be neglected as 1 mm amberlyst beads have the same activity as the powdered catalyst (thus, the activity is independent of the fluid–solid interfacial area). The solid catalyst can be recycled several times without loss in activity.

Overall, the selectivity towards benzaldehyde (PhCHO) is very high, ranging from 95% at 80°C to 98.5% at 60°C . The most important by-products are benzyl nitrite, 2-benzyl-1,3-dioxolane (from acetalization of benzaldehyde with 1,2-dihydroxyethane, formed in the acid catalyzed decomposition

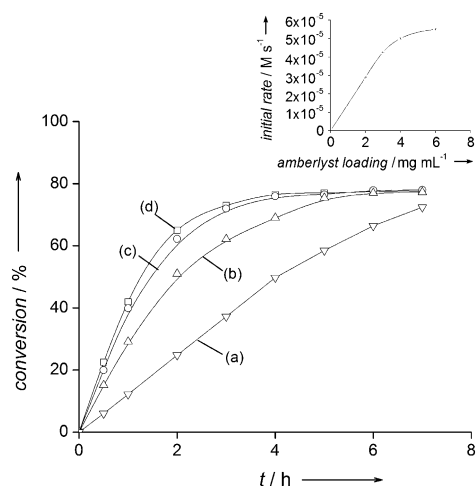


Figure 2. PhCH_2OH conversion versus time for various amounts of amberlyst: a–d): 50, 75, 100, and 150 mg (5 mm NaNO_2). The insert shows the dependency of the initial rate on the amberlyst amount.

of 1,4-dioxane^[17], and benzoic acid (Figure 3). Interestingly, benzyl nitrite (PhCH_2ONO) can be identified as a reaction intermediate: its concentration initially increases, then decreases. The benzyl nitrite is formed in the equilibrated esterification reaction $\text{PhCH}_2\text{OH} + \text{HNO}_2 \rightleftharpoons \text{PhCH}_2\text{ONO} + \text{H}_2\text{O}$. Traces of benzyl nitrate, benzyl benzoate, dibenzylether, and benzyl formate (formed out of PhCH_2OH and formic acid, a decomposition product of 1,4-dioxane^[18]) are detected by GC-MS. The most important by-products arise from the use of dioxane as solvent and can be avoided when working in pure PhCH_2OH . Note that the maximum benzyl nitrite concentration is significantly higher at lower reaction temperatures (e.g. 34 mM at 60°C versus 21 mM at 80°C); when the reaction is performed with less amberlyst (e.g. 50 mg instead of 150 mg), the benzyl nitrite concentration remains below the GC-MS detection limit.

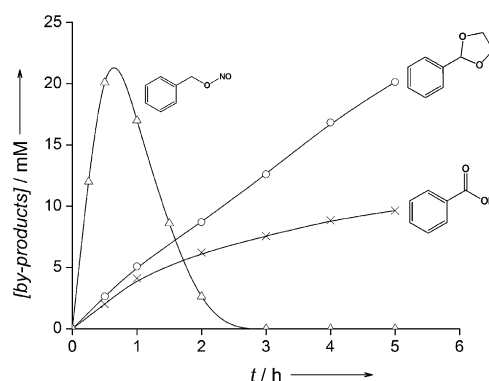


Figure 3. Time evolution of the most important by-products at 80°C under standard conditions ($[\text{PhCH}_2\text{OH}]_0 = 500\text{ mM}$, $[\text{NaNO}_2]_0 = 5\text{ mM}$, $[\text{HNO}_3]_0 = 125\text{ mM}$, 150 mg of amberlyst and 1 atm O_2).

Doubling the initial alcohol concentration barely affects the rate at low amberlyst loadings, whereas first-order behavior is observed for higher catalyst loadings. Addition

of conventional radical trappers, such as 2,4,6-tri-*tert*-butylphenol, did not significantly affect the reaction rate or selectivity, excluding the involvement of peroxy or alkoxy radicals as important reaction intermediates.

Mass spectrometry was used to monitor the evolution of NO (m/z 30) and N₂O (m/z 44) in the gas phase. N₂O was also monitored with transmission IR spectroscopy of the gas phase under static O₂ pressure of 1 atm (Figure 4; ν_3 vibrational

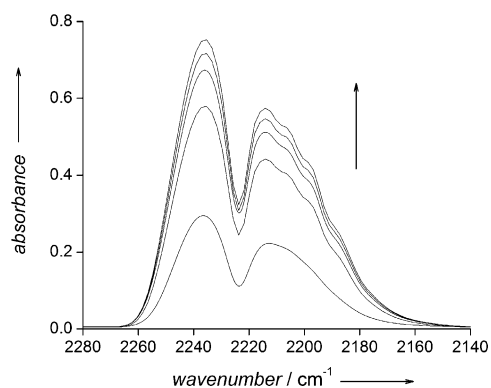


Figure 4. Gas-phase transmission IR spectra from a reaction performed at 80 °C under static O₂ pressure of 1 atm (spectra shown after 0.5, 1, 2, 3, and 5 h; see Supporting Information): ν_3 vibrational mode of N₂O.

mode), unambiguously assigning the m/z signal of 44 to nitrous oxide. No signal for nitric oxide was observed at 1876 cm⁻¹, probably due to the small dipole-moment change of the NO-stretch. Despite the yellow color of the liquid and the m/z signal of 46 determined in the liquid phase, no NO₂ could be detected in the gas phase, confirming that it is strongly absorbed in the dioxane solution. The addition of water to the reaction mixture (in addition to the water already added in the 65 % HNO₃ solution) prevents the formation of the yellow color and inhibits the reaction. Presumably, water traps NO₂ in Reaction (2). This observation suggests NO₂ as an important reaction intermediate.

Figure 5 shows the temperature dependence of the overall oxidation reaction catalyzed by 6 mg amberlyst per mL. The

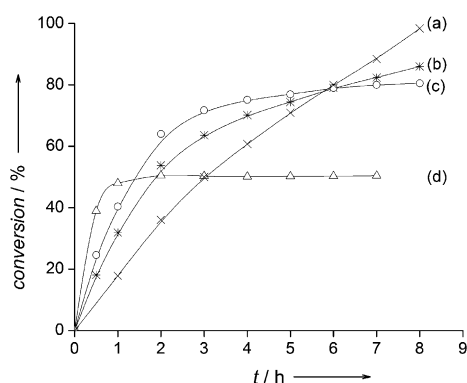


Figure 5. Temperature dependency of the PhCH₂OH conversion in the presence of 5 mM NaNO₂ under standard conditions (a–d: 60, 70, 80, and 90 °C, respectively).

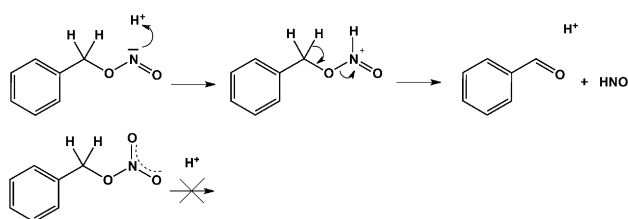
corresponding Arrhenius activation energy of (12 ± 1) kcal mol⁻¹ excludes mass-transfer limitations as an explanation for the leveling off in reaction rate at higher amberlyst loadings (see Figure 2). Using only 2 mg amberlyst per mL, the activation energy is significantly higher, (33 ± 1) kcal mol⁻¹. This observation, together with a change in reaction order in alcohol (see above), points towards a shift in rate-determining-step when going from a low-to-high amberlyst loading. Interestingly, a higher end-conversion can be achieved at lower temperature.

To understand the precise role of the benzyl nitrite ester (PhCH₂ONO)—experimentally identified as a reaction intermediate (see above)—we synthesized it according to a literature procedure^[19] and studied its acid-catalyzed decomposition (see Supporting Information). A stoichiometric amount of benzaldehyde is formed, confirming that the nitrite ester is a pivotal intermediate. The reaction is first-order in both nitrite and amberlyst. In the temperature range 40–70 °C, the rate constant is well described by the Arrhenius expression $(3 \pm 2) \times 10^6 \exp(-13 \pm 1 \text{ kcal mol}^{-1}/RT) \text{ M}^{-1} \text{ s}^{-1}$. During the nitrite decomposition—performed under N₂ atmosphere—N₂O formation is detected by IR spectroscopy, identifying this step as the nitrous oxide source. Although the initial nitrite decomposition rate is not affected by the presence of NO₂, at higher reaction times, NO₂ slightly enhances the decomposition rate, due to the formation of HNO₃ and HNO₂ in Reaction (2) which increases the proton (i.e. the catalyst) concentration. More important is that approximately 20 % less N₂O was found in the gas phase when the nitrite decomposition was studied in a dioxane solution saturated with 0.5 % NO₂ in an He gas flow, prior to the addition of amberlyst. Benzyl nitrate (PhCH₂ONO₂), although being detected with GC-MS as a trace product, was found to be unreactive at 80 °C for several hours and should hence be considered as a spectator in equilibrium with PhCH₂OH plus HNO₃, rather than a true reaction intermediate.

Note that at high amberlyst loadings (i.e., 6 mg mL⁻¹), the observed activation energy (i.e. (12 ± 1) kcal mol⁻¹) corresponds with the activation energy of the nitrite decomposition (i.e. (13 ± 1) kcal mol⁻¹, see above). This agreement, together with the observed first-order in alcohol, is an important indication that this acid-catalyzed decomposition of the nitrite ester (formed by PhCH₂OH + HNO₂ ⇌ PhCH₂ONO + H₂O) is the rate-determining-step (RDS) in the overall mechanism, at least at high catalyst loadings. This hypothesis explains why the reaction rate levels off after the nitrite intermediate reaches its maximum concentration (i.e. after 1 h, see curve b in Figure 1 and Figure 2). Under the assumption that the nitrite decomposition is rate-determining, the rate constant of this decomposition can be estimated from the overall reaction rate (e.g. 0.26 M h⁻¹ after 0.5 h, see curve b in Figure 1), the corresponding nitrite and proton concentration stemming from amberlyst (i.e. [nitrite] = 20 mM, see Figure 2, and [H⁺]_{amberlyst} = 28 mM) to be (0.13 ± 0.03) M⁻¹ s⁻¹. This value is in excellent agreement with the value obtained from our nitrite decomposition study (see Supporting Information), (0.11 ± 0.02) M⁻¹ s⁻¹.

At low amberlyst loadings (i.e., 2 mg mL⁻¹), HNO₃ decomposition (according to the stoichiometry of Reaction (1)) is likely to be the RDS, explaining the zero order in alcohol. The experimental activation energy in this range (i.e. 33 ± 1 kcal mol⁻¹) is significantly lower than the reported HNO₃ self-decomposition barrier of 38.7 kcal mol⁻¹,^[20] pointing towards an amberlyst-catalyzed decomposition (see Supporting Information). This shift in RDS also explains why the nitrite ester could not be detected when the reaction is performed with a low amberlyst loading (see above) as its decomposition is faster than its formation.

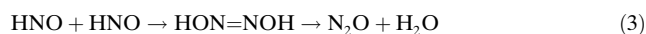
All these experimental observations point towards an acid-catalyzed decomposition of the nitrite ester, involving the protonation of the N-atom (Scheme 1), leading to the



Scheme 1. Acid-catalyzed decomposition of PhCH₂ONO to PhCHO and HNO; PhCH₂ONO₂ seems unreactive under similar conditions.

formation of HNO. Because the nitrate ester cannot be protonated it is unreactive under similar reaction conditions.

HNO is a reactive substance that dimerizes very rapidly to hyponitrous acid (HON=NOH) which decomposes to water and N₂O [Reaction (3)].^[21] The overall rate constant for Reaction (3) can be described by $k_3(T) = 6.9 \times 10^5 \exp(-2.8 \text{ kcal mol}^{-1}/RT) \text{ M}^{-1} \text{ s}^{-1}$.^[22] In the presence of NO₂, HNO can be converted into NO (detected by mass spectrometry) by Reaction (4), regenerating HNO₂.



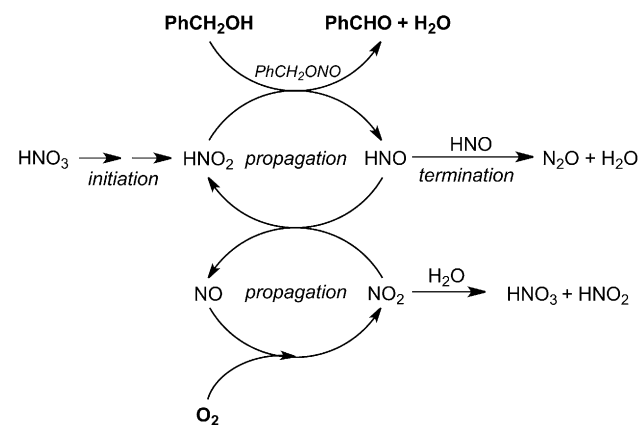
Reaction (4) is driven by the weak H–NO bond of only 49 kcal mol⁻¹, leading to a $k_4(T) = 6 \times 10^8 \exp(-2 \text{ kcal mol}^{-1}/RT) \text{ M}^{-1} \text{ s}^{-1}$.^[23] Kinetic competition between Reactions (3) and (4) explains why less N₂O is formed during nitrite decomposition in the presence of NO₂ (see above). If water is added to the reaction mixture, NO₂ is rapidly trapped by Reaction (2), preventing it from reacting with HNO and the reaction is quenched (see above).

NO can be re-oxidized by O₂ to NO₂ according to Reaction (5).^[22] In the absence of O₂, NO can probably also react with HNO₃,^[24] regenerating HNO₂ and NO₂ [Reaction (6)], explaining why even under an inert N₂ atmosphere a $\Delta[\text{PhCH}_2\text{OH}]/[\text{HNO}_3]_0 \approx 2$ can be achieved. Note that rapid re-oxidation of NO to NO₂ is crucial to prevent HNO from dimerizing and forming N₂O. This explains why a higher end-conversion can be reached at higher O₂ pressure, given a certain temperature (see Figure 1).



Note that, although the temperature dependence of HNO consumption by Reactions (3) and (4) are similar, HNO formation (by nitrite decomposition) is more accelerated at higher temperature than NO₂ formation by Reaction (5) which actually becomes slower at higher *T*.^[22] This hypothesis is confirmed by the lower nitrite ester concentration at higher temperatures. Because of this situation, the [HNO]/[NO₂] concentration ratio will increase at increasing temperature, favoring N₂O formation (termination) as seen by IR spectroscopy. As an example, at 90 °C, 40% more N₂O is found than at 80 °C, both at 60% alcohol conversion. This explains why a higher end conversion can be achieved at a lower *T* (see Figure 5).

Scheme 2 summarizes the mechanistic insights. It shows the NO_x and HNO_x cycling and emphasizes that O₂ is the terminal oxidant; HNO₃ only triggers an aerobic oxidation cycle.



Scheme 2. HNO₃ is initiating a NO_x/HNO_x mediated oxidation cycle.

As reported above, water has a detrimental effect on the reaction as it traps the NO₂ in Reaction (2) and hence favors the formation of N₂O. We suspect this effect limits the TON in (H)NO_x under conditions when the nitrite decomposition is rate-determining (i.e., high amberlyst loadings and hence high reaction rates). Karl–Fischer titration of H₂O in the system shows a gradual increase of the water content from approximately 0.5 w% just after addition of the HNO₃ to 1.8 w% after 6 h (corresponding to 80% conversion).

This observation prompted us to remove water in situ. Addition of molecular sieves to the reaction resulted in inhibition, probably due to strong adsorption of (H)NO_x, present in the liquid phase. Therefore a gas recirculation reactor was constructed (Figure 6) in which the gas phase is constantly pumped over a fix-bed with molecular sieve 4 Å to remove the water via the gas phase.

Using this set-up it is possible to significantly speed up the reaction, while also increasing the end conversion to 100% (Figure 7). Karl–Fischer titration confirms that this gas

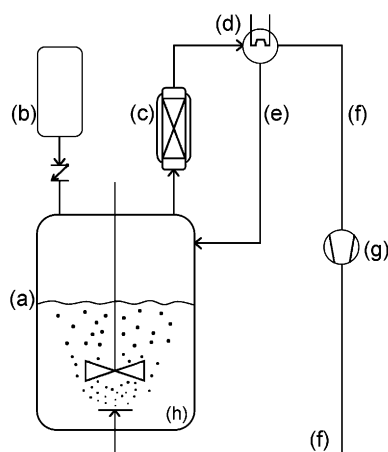


Figure 6. Gas recirculation reactor: a) heated tank-reactor, b) O₂ reservoir connected to reactor by a check-valve, c) jacketed packed column with 4 Å molecular sieves (kept at reaction temperature to avoid solvent condensation), d) condenser, e) condensate recycling, f) dried-gas recycling, g) membrane pump, and h) gas disperser.

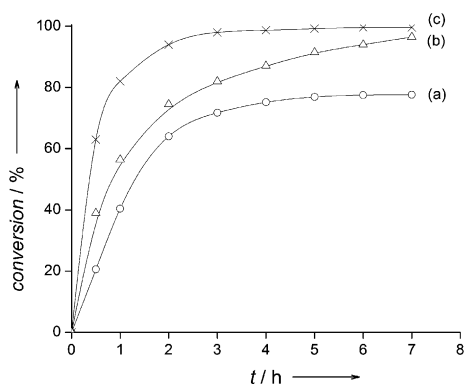


Figure 7. PhCH₂OH conversion in the presence of 5 mm NaNO₂ at 80 °C versus time for a reaction performed in a) a bubble column reactor and in the gas recirculation reactor with drying of the gas phase (gas recirculation rate of b) 75 and c) 150 mL min⁻¹).

recirculation reactor limits the water content to 0.5 w%. It is important to emphasize that the observed effect is not due to enhanced gas–liquid mass-transfer as increasing the O₂ superficial flow rate in a bubble column reactor, or operating the gas recirculation reactor without molecular sieve, did not lead to an improvement.

From this study, it can be concluded that HNO₃ is able to start off a chain oxidation of benzyl alcohol, mediated by (H)NO_x species; O₂ is however the terminal oxidant. HNO₂ reacts with the alcohol substrate to form a nitrite ester which decomposes, acid catalyzed, to the benzaldehyde product and HNO. The reaction of HNO with NO₂, regenerates HNO₂ and forms NO which is oxidized to NO₂ (propagation reactions). HNO can dimerize and yield N₂O in a termination reaction. A significant increase in chain length, and hence an improved yield, can be achieved at lower temperature, or upon drying of the gas phase. This chain reaction is catalyzed by the solid acid amberlyst-15. Depending on the acid catalyst loading, either the HNO₃ or the nitrite decomposition is rate determining;

both steps are acid catalyzed. These mechanistic insights will be used as a starting point to investigate other HNO₃-based oxidation reactions, such as adipic acid synthesis. The present study shows that the reaction of the alcohol substrate with HNO₂ leads to the reactive (H)NO_x species. Most likely this is the reason why cyclohexanol is needed as a (co-)substrate in the adipic acid synthesis as pure cyclohexanone is rather inert under the same conditions.^[7]

Experimental Section

Standard experiments were carried out in a bubble column reactor using 1,4-dioxane (25 mL; Fluka, p.a. ≥ 99.5%) as a solvent, PhCH₂OH (500 mm; Acros, 99%), HNO₃ (125 mm; Merck, p.a. 65%), NaNO₂ (5 mm; Sigma–Aldrich, ≥ 99%), and amberlyst-15 (150 mg; Sigma–Aldrich). High-pressure reactions were performed in a 100 mL stainless steel Parr reactor equipped with a glass insert and a polyether ether ketone (PEEK) propeller. Products were quantified using GC (HP-FFAP column, Flame-Ionization-Detector), or—in the case of the thermally unstable nitrite—with GC-MS with cool-on-column injection (HP-5 column). More information on the experimental procedures can be found in the ESI.

Received: August 8, 2011

Published online: October 21, 2011

Keywords: alcohols · nitric acid · oxidation · reaction kinetics · selectivity

- [1] F. Cavani, J. H. Teles, *ChemSusChem* **2009**, *2*, 508–534.
- [2] G. Franz, R. Sheldon, *Oxidation, Ullmann's Encycl. Ind. Chem.*, Wiley-VCH, Weinheim, **2000**.
- [3] See, for example, a) I. Hermans, T. L. Nguyen, P. A. Jacobs, J. Peeters, *ChemPhysChem* **2005**, *6*, 637–645; b) I. Hermans, P. A. Jacobs, J. Peeters, *Chem. Eur. J.* **2006**, *12*, 4229–4240; c) U. Neuenschwander, F. Guignard, I. Hermans, *ChemSusChem* **2010**, *3*, 75–84.
- [4] M. Thiemann, E. Scheibler, K. W. Wiegand, *Nitric Acid, Nitrous Acid, and Nitrogen Oxides, Ullmann's Encycl. Ind. Chem.*, Wiley-VCH, Weinheim, **2000**.
- [5] C. Seidel, BASF expands methanesulfonic acid plant in Ludwigshafen, Press Information, May 11th **2010**.
- [6] See, for example, H. Osato, M. Kabaki, S. Shimizu, *Org. Process Res. Dev.* **2011**, *15*, 581–584, and references therein.
- [7] M. T. Musser, *Adipic Acid, Ullmann's Encycl. Ind. Chem.*, Wiley-VCH, Weinheim, **2000**.
- [8] a) I. Hermans, K. Janssen, B. Moens, A. Philippaerts, B. Van Berlo, J. Peeters, P. A. Jacobs, B. F. Sels, *Adv. Syn. Catal.* **2007**, *349*, 1604–1608, and references therein; b) K. Banert, O. Plefka, *Angew. Chem.* **2011**, *123*, 6295–6298; *Angew. Chem. Int. Ed.* **2011**, *50*, 6171–6174.
- [9] A. Levina, S. Trusov, *J. Mol. Catal.* **1994**, *88*, L121–L123.
- [10] a) Y. Kuang, N. M. Islam, Y. Nabae, T. Hayakawa, M. Kakimoto, *Angew. Chem.* **2010**, *122*, 446–450; *Angew. Chem. Int. Ed.* **2010**, *49*, 436–440; b) Y. Kuang, H. Rokubuichi, Y. Nabae, T. Hayakawa, M. Kakimoto, *Adv. Synth. Catal.* **2010**, *352*, 2635–2642.
- [11] a) F. Bleger, O. Simon, A. Schouteeten, WO 2009/092734, **2009**; b) F. Bleger, O. Simon, A. Schouteeten, US 2011/0012056A1, **2011**.
- [12] a) Y. Ogata, Y. Sawaki, F. Matsunaga, H. Tezuka, *Tetrahedron* **1966**, *22*, 2655–2664; b) D. S. Ross, C.-L. Gu, G. P. Hum, R. Malhotra, *Int. J. Chem. Kinet.* **1986**, *18*, 1277–1288; c) S. R. Joshi, K. L. Kataria, S. B. Sawant, J. B. Joshi, *Ind. Eng. Chem. Res.* **2005**, *44*, 325–333.

- [13] I. Hermans, J. Peeters, L. Vereecken, P. Jacobs, *ChemPhysChem* **2007**, *8*, 2678–2688.
- [14] Y. Wada, K. Morimoto, T. Goibuchi, H. Tomiyasu, *Radiochim. Acta* **1995**, *68*, 233–243.
- [15] A. I. Kazakov, Yu. I. Rubtsov, L. P. Andrienko, G. B. Manelis, *Russ. Chem. Bull.* **1987**, *36*, 1999–2002.
- [16] Y. Kameoka, R. L. Pigford, *Ind. Eng. Chem. Fundam.* **1977**, *16*, 163–169.
- [17] K. P. C. Vollhardt, N. E. Shore, *Organic Chemistry Structure and Function*, 4th ed., Freeman, New York, **2002**.
- [18] M. A. Beckett, I. Hua, *Environ. Sci. Technol. Environ. Sci. Technol.* **2000**, *34*, 3944–3953.
- [19] M. P. Doyle, J. W. Terpstra, R. A. Pickering, D. M. LePaire, *J. Org. Chem.* **1983**, *48*, 3379–3382.
- [20] H. F. Cordes, N. R. Fetter, J. A. Happe, *J. Am. Chem. Soc.* **1958**, *80*, 4802–4808.
- [21] V. Shafirovich, V. S. Lyman, *Proc. Natl. Acad. Sci. USA* **2002**, *99*, 7340–7345.
- [22] NIST Chemical Kinetics Database, <http://kinetics.nist.gov/kinetics/>.
- [23] W. Tsang, J. T. Herron, *J. Phys. Chem. Ref. Data* **1991**, *20*, 609–663.
- [24] R. Svensson, E. Ljungström, *Int. J. Chem. Kinet.* **1988**, *20*, 857–866.
-